Developmental Biology 417 (2016) 104–113

Contents lists available at ScienceDirect

Developmental Biology

journal homepage: www.elsevier.com/locate/developmentalbiology

Evolution of Developmental Control Mechanisms

Smads and insect hemimetabolan metamorphosis

Carolina G. Santos [1], Ana Fernandez-Nicolas [1], Xavier Belles *

Institut de Biologia Evolutiva (CSIC-Universitat Pompeu Fabra), Passeig Marítim 37, 08003 Barcelona, Spain

ARTICLE INFO

Article history:
Received 14 April 2016
Received in revised form
7 July 2016
Accepted 12 July 2016
Available online 21 July 2016

Keywords:
Medea
Mad
Smox
Insect metamorphosis
Blattella
Smads
Bursicon

ABSTRACT

In contrast with *Drosophila melanogaster*, practically nothing is known about the involvement of the TGF-β signaling pathway in the metamorphosis of hemimetabolan insects. To partially fill this gap, we have studied the role of Smad factors in the metamorphosis of the German cockroach, *Blattella germanica*. In *D. melanogaster*, Mad is the canonical R-Smad of the BMP branch of the TGF-β signaling pathway, Smox is the canonical R-Smad of the TGF-β/Activin branch and Medea participates in both branches. In insects, metamorphosis is regulated by the MEKRE93 pathway, which starts with juvenile hormone (JH), whose signal is transduced by Methoprene-tolerant (Met), which stimulates the expression of Krüppel homolog 1 (Kr-h1) that acts to repress E93, the metamorphosis trigger. In *B. germanica*, metamorphosis is determined at the beginning of the sixth (final) nymphal instar (N6), when JH production ceases, the expression of Kr-h1 declines, and the transcription of E93 begins to increase. The RNAi of Mad, Smox and Medea in N6 of *B. germanica* reveals that the BMP branch of the TGF-β signaling pathway regulates adult ecdysis and wing extension, mainly through regulating the expression of bursicon, whereas the TGF-β/Activin branch contributes to increasing E93 and decreasing Kr-h1 at the beginning of N6, crucial for triggering adult morphogenesis, as well as to regulating the imaginal molt timing.

1. Introduction

The transforming growth factor-β (TGF-β) signaling pathway is fundamental for controlling developmental programs and cell behavior in animals (Herpin et al., 2004). The TGF-β ligand proteins bind to Ser/Thr kinase receptors and generally transduce the signal through Smad transcription factors (Massague, 2012; Moustakas and Heldin, 2009). There are two Ser/Thr kinase receptor types, type I and type II, which typically form a tetramer receptor complex comprising two type I and two type II receptors. Type I transmit information from outside to inside the cell by binding extracellular ligands and phosphorylating intracellular transcription factors. Type II receptors are constitutively active kinases that phosphorylate and activate the type I when forming a complex with them through ligand binding. Receptor-activated (R-) Smad proteins are the most typical transcription factors phosphorylated by type I receptors. Upon receptor-induced phosphorylation, R-Smads typically form complexes with a common-mediator (Co-) Smad, and the complex is translocated to the nucleus where, in cooperation with other transcription factors, it contributes to regulating (co-activating or co-repressing) the transcription of target genes (Heldin and Moustakas, 2012). These Smad complexes in turn induce the expression of the inhibitory (I) Smads that negatively regulate the strength and duration of the signal (Itoh and ten Dijke, 2007).

All TGF-β signaling pathways can be classified into two branches, the TGF-β/Activin branch and the Bone Morphogenetic Protein (BMP) branch, based on the specificity of interaction between the L45 loop of the type I receptor and the L3 loop of the MH2 domain of the R-Smads. The TGF-β/Activin branch signals through Smad 2 and Smad 3, whereas the BMP branch signals through Smad 1, Smad 5 and Smad 8; in both cases the Co-Smad is Smad 4, whereas Smad 6 and Smad 7 are I-Smads (Moustakas and Heldin, 2009). The most thoroughly studied insect species is the fly *Drosophila melanogaster*, where the TGF-β/Activin branch operates through the type I receptor babo and signals through a single R-Smad (Smox, ortholog of Smad 2/3) and a single Co-Smad (Medea, ortholog of Smad 4), whereas the BMP branch has two type I receptors: thick veins (tkv) and saxophone (sax), although it also operates through a single R-Smad (Mad, ortholog of Smad 1/5/8) and Medea. A single I-Smad (Dad, ortholog of Smad 6/7) acts in both branches of the TGF-β signaling pathway in this fly (Peterson and O'Connor, 2014).

While the importance of the TGF-β signaling pathways in *D. melanogaster* has been comprehensively shown in embryogenesis (Peterson and O'Connor, 2014), reports concerning postembryonic development are limited to a few case studies. In the BMP branch, the data refers to a handful of downstream targets that participate in wing formation, like *spalt* (*sal*), *optomotor blind* (*omb*), *vestigial*

* Corresponding author.
E-mail address: xavier.belles@ibe.upf-csic.es (X. Belles).
[1] These authors have contributed equally.

http://dx.doi.org/10.1016/j.ydbio.2016.07.006
0012-1606/

(*vg*) and *larval translucida* (*ltl*) (de Celis et al., 1996; Grimm and Pflugfelder, 1996; Kim et al., 1996; Szuperak et al., 2011). The TGF-β/Activin branch has been shown to be involved in wing disc patterning (Peterson et al., 2012; Peterson and O'Connor, 2013) and neuronal remodeling (Zheng et al., 2003), as well as the regulation of the metamorphic molt timing by influencing ecdysone production (Brummel et al., 1999; Gibbens et al., 2011).

In contrast with *D. melanogaster*, practically nothing is known about the involvement of the TGF-β signaling pathways in the metamorphosis of hemimetabolan insects. This lack of information in less-modified insect species prevents comparisons and hypotheses being made regarding the possible changing roles of these pathways through insect evolution and, in particular, their influence on the evolution of insect metamorphosis from hemimetaboly to holometaboly (Belles, 2011). To partially fill this gap, we have studied the role of Smad factors in the metamorphosis of the German cockroach, *Blattella germanica*. A previous analysis of tergal gland transcriptomes (Ylla and Belles, 2015) have revealed the expression of a number of genes related to the TGF-β signaling pathways, including those expressing Smads, decapentaplegic (dpp), omb, tkv, vg and spalt, for example. The tergal gland of male cockroaches is a structure that secretes attractant substances that facilitate mating and is formed during adult morphogenesis (Ylla and Belles, 2015). Thus, the occurrence of Smad transcripts suggests that TGF-β signaling pathways contribute to the morphogenesis of the tergal gland, and of the adult, in general.

In *B. germanica*, as in other insect species, two principal hormones are involved in postembryonic development and metamorphosis. One of these is ecdysone, which promotes the successive molts that allow growth, and the other is juvenile hormone (JH), which represses metamorphosis (Nijhout, 1994) during juvenile stages, and whose decrease in the pre-adult stage triggers it. The molecular details of this juvenile-adult transition have been elucidated recently and can be summarized in what has been called the MEKRE93 pathway (Belles and Santos, 2014; Jindra et al., 2015), which essentially switches on and off metamorphosis in all studied insect species. According to this pathway, and with reference to *B. germanica*, in pre-final nymphal instars the JH signal is transduced by Met (Lozano and Belles, 2014) and Taiman (Lozano et al., 2014), and stimulates the expression of Kr-h1, the master repressor of metamorphosis (Lozano and Belles, 2011). Under these conditions the molts proceed in the sense nymph-nymph. At the beginning of the final instar nymph, JH production ceases (Treiblmayr et al., 2006), Kr-h1transcription begins to decline (Lozano and Belles, 2011), and the expression of E93, that had been repressed by Kr-h1 (Belles and Santos, 2014), begins to increase significantly, while repressing the expression of Kr-h1 (Belles and Santos, 2014; Ureña et al., 2014). Then, the molt proceeds in the sense nymph-adult. The purpose of the present work was to study whether the TGF-β signaling pathway contributes to regulating the metamorphosis of *B. germanica*, with a particular focus on possible interplay with the MEKRE93 pathway.

2. Results

2.1. Depletion of Mad impairs the imaginal ecdysis and wing extension in the adult

By combining a BLAST search on *B. germanica* tergal gland transcriptomes, mapping the resulting sequence in the *B. germanica* genome, and PCR strategies, we obtained a cDNA of 1419 bp comprising a complete ORF whose conceptual translation rendered a 473 amino acid protein with significant sequence similarity to Mad orthologs of other organisms (top BLAST scores were obtained from Mad or Smad 1, 5 or 8). The sequence (GenBank accession number LN901331) contains the MH1 and MH2 domains typical of Smad proteins (Heldin and Moustakas, 2012), connected by the linker region. The expression pattern of this *B. germanica* Mad was determined using qRT-PCR on tergites 7 and 8 (T7–8, which metamorphose into the tergal gland in the adult), as well as tergites 4 and 5 (T4–5, which do not show metamorphosis in the adult) of male fifth (N5) and sixth (N6) nymphal instars. The expression levels were relatively high and similar in T7–8 and T4–5, oscillating between 5 and 25 mRNA copies per 1000 copies of Actin-5c mRNA. The values were high at the beginning of the stage and then progressively decreased. In N6 the levels were more constant, clearly decreasing only on the last day (Fig. 1A).

To study the roles of Mad in metamorphosis we used RNAi approaches, by designing a dsRNA encompassing the linker region (360 nucleotides) and part of the MH1 domain (171 additional nucleotides) of Mad (dsMad). We injected two doses of 1 μg each of dsMad into male nymphs, one into freshly emerged penultimate instar (N5D0), and the other into freshly emerged final instar (N6D0). Controls received the same treatment but with dsMock. All dsMock-treated specimens (n=33) molted to normal N6 and then to normal adults. Of the dsMad-treated specimens (n=71), all molted to normal N6, and then 31 (43%) molted to adults but without completing the ecdysis, thus dying trapped in the exuvium; 27 (38%) also had ecdysis problems but finally molted to adults that showed completely unextended wings, and 13 (19%) molted to adults with partially extended wings, especially in the apical part, with the tegmina longitudinally curled and tile-shaped, as if they were "inflated", and the membranous wings also not well extended, especially in the apical part (Fig. 1B). Transcript measurements carried out on the complete set of tergites on N6D1 and N6D4 showed that Mad mRNA levels were significantly reduced (an average of 84% and 88%, respectively) in dsMad-treated specimens, whereas those of Medea and Smox were unaffected (Fig. 1C), indicating that depletion was Mad-specific.

The ecdysis problems observed in Mad-depleted specimens are reminiscent of those found when depleting the mRNA levels of members of the ecdysone signaling pathway, like HR3A (Cruz et al., 2007). Thus, on N6D6, when the levels of ecdysone reach a peak in the hemolymph (Romaña et al., 1995), we measured the expression of HR3A in the complete set of tergites from Mad-depleted specimens. The results indicated that there were no differences between dsMad-treated insects and the controls (Fig. 1D). Then, as the ecdysis defects were observed only in the metamorphic molt, we examined the expression of Kr-h1 and E93, two final components of the MEKRE93 pathway (Belles and Santos, 2014), on N6D1 and N6D4. Results showed that neither Kr-h1 nor E93 expression was significantly affected by the dsMad treatment (Fig. 1E).

2.2. Depletion of Smox disrupts the MEKRE93 pathway and delays the imaginal molt

Equivalent BLAST-PCR approaches rendered a partial cDNA of Smox, comprising 1034 bp containing, approximately, the 5′ half of the ORF (540 nucleotides) including a part of the MH2 domain, and 494 nucleotides corresponding to the 3′UTR (GenBank accession number LT575495). A conceptual translation of the partial ORF gave a 180 amino acid sequence which was significantly similar to *D. melanogaster* Smox or Smad 2/3 orthologs of other species. Smox mRNA levels were relatively low, oscillating between 2 and 10 mRNA copies per 1000 copies of Actin-5c mRNA. In N5 the pattern was similar to that of Mad: high expression levels at the beginning of the stage that progressively decreased during it. The N6 pattern was the same as for N5, with highest levels occurring just after the molt (Fig. 2A).

RNAi approaches were also followed in order to functionally

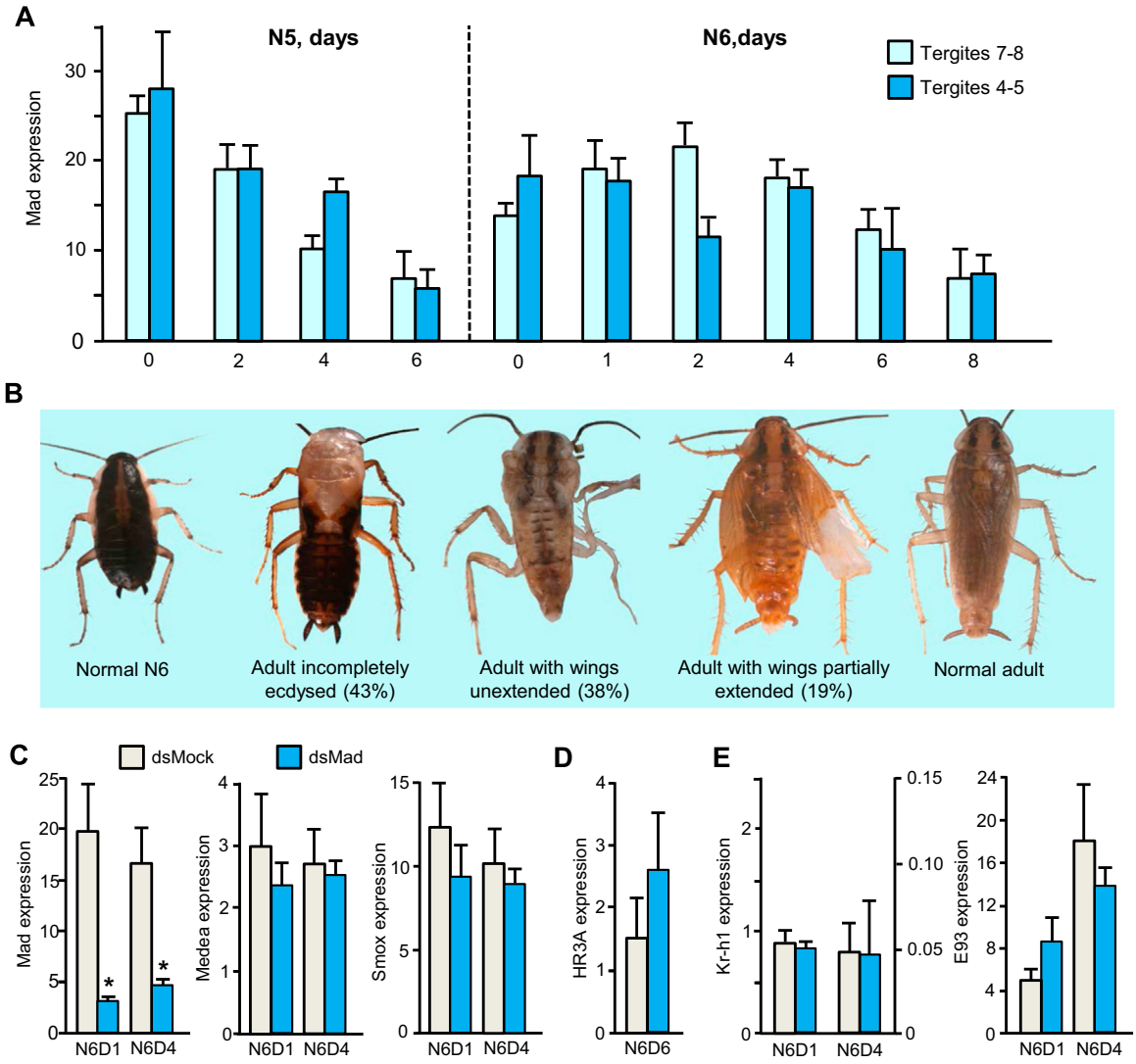

Fig. 1. Expression and function of Mad during metamorphosis of *Blattella germanica*. (A) Mad mRNA levels in fifth and sixth instars of male nymphs (N5 and N6, respectively), in tergites 7 and 8 and tergites 4 and 5. (B) Dorsal view of specimens resulting from dsMad and dsMock (control) treatments. Normal N6, normal adult and phenotypes obtained with dsMad treatments; specimens were treated with two doses of 1 μg each of dsMad on male nymphs, one on N5D0 and the other on N6D0. (C) Mad, Smox and Medea mRNA levels in dsMad-treated and controls, measured on N6D1 and N6D4. (D) HR3A mRNA levels on N6D6. (E) Kr-h1 and E93 mRNA levels on N6D1 and N6D6; the scale or ordinates on the right of the Kr-h1 histogram applies for N6D4. From (C) to (E), mRNA levels were measured in the complete set of tergites. Each point of quantitative data in histograms represents between 3 and 5 biological replicates; results represent copies of the given transcript per 1000 copies of BgActin-5c mRNA and are expressed as the mean ± SEM; the asterisks indicate statistically significant differences with respect to controls ($p < 0.05$), according to the REST software tool (Pfaffl et al., 2002).

study Smox. The dsRNA designed encompassed 387 nucleotides in the 3′UTR region of Smox mRNA (dsSmox). We injected two doses of 2 μg each of dsSmox into male nymphs, one on N5D0 and the other on N6D0. The controls received the same treatment but with dsMock. All dsMock-treated specimens (n=38) molted to normal N6 and then normal adults. Similarly, all dsSmox-treated specimens (n=49), molted to normal N6, and then to adults that were morphologically normal. However, the timing of the molt in N6 (not in N5) was significantly delayed with respect to the dsMock control group (Fig. 2B). Transcript measurements carried out on the complete set of tergites on N6D1 and N6D4 indicated that Smox mRNA levels were significantly reduced (an average of 39% and 38%, respectively) in dsSmox-treated specimens, whereas those of Medea and Mad were unaffected (Fig. 2C).

To confirm that the molting peak of ecdysone did not occur at the right time, we measured the expression of HR3A, in the complete set of tergites from Smox-depleted specimens on N6D6. The results indicated that HR3A was well expressed in controls, whereas expression was very low in dsSmox-treated, in both N6D6 and three days later, in N6D9 (Fig. 2D). We also examined the effects of Smox depletion on Kr-h1 and E93 expression on N6D1 and N6D4. Interestingly, the results indicated that dsSmox treatment impaired the decrease of Kr-h1 expression that normally occurs in N6D1, as the mRNA levels were significantly higher than those of the controls. In N6D4, whereas the mRNA levels of Kr-h1 were very low, ca. 0.05 copies per 1000 copies of Actin-5c mRNA, those of Smox-depleted specimens were still around 0.13 copies per 1000 copies of Actin-5c mRNA, on average. Moreover, on N6D1 the levels of E93 mRNA were significantly lower in dsSmox-treated specimens, whereas on N6D4, they still tended to be lower in the Smox-depleted group than in the controls (Fig. 2E).

As Kr-h1 and E93 are reciprocally repressed (Belles and Santos, 2014), the results suggest that Smox could either co-repress Kr-h1 or co-activate E93 (or both). To shed light on this disjunctive, we treated Smox-depleted animals with JH. Given that JH efficiently induces Kr-h1 expression (Lozano and Belles, 2011), if the first conjecture were true, then the JH-driven increase of Kr-h1 expression would be more dramatic in Smox-depleted specimens.

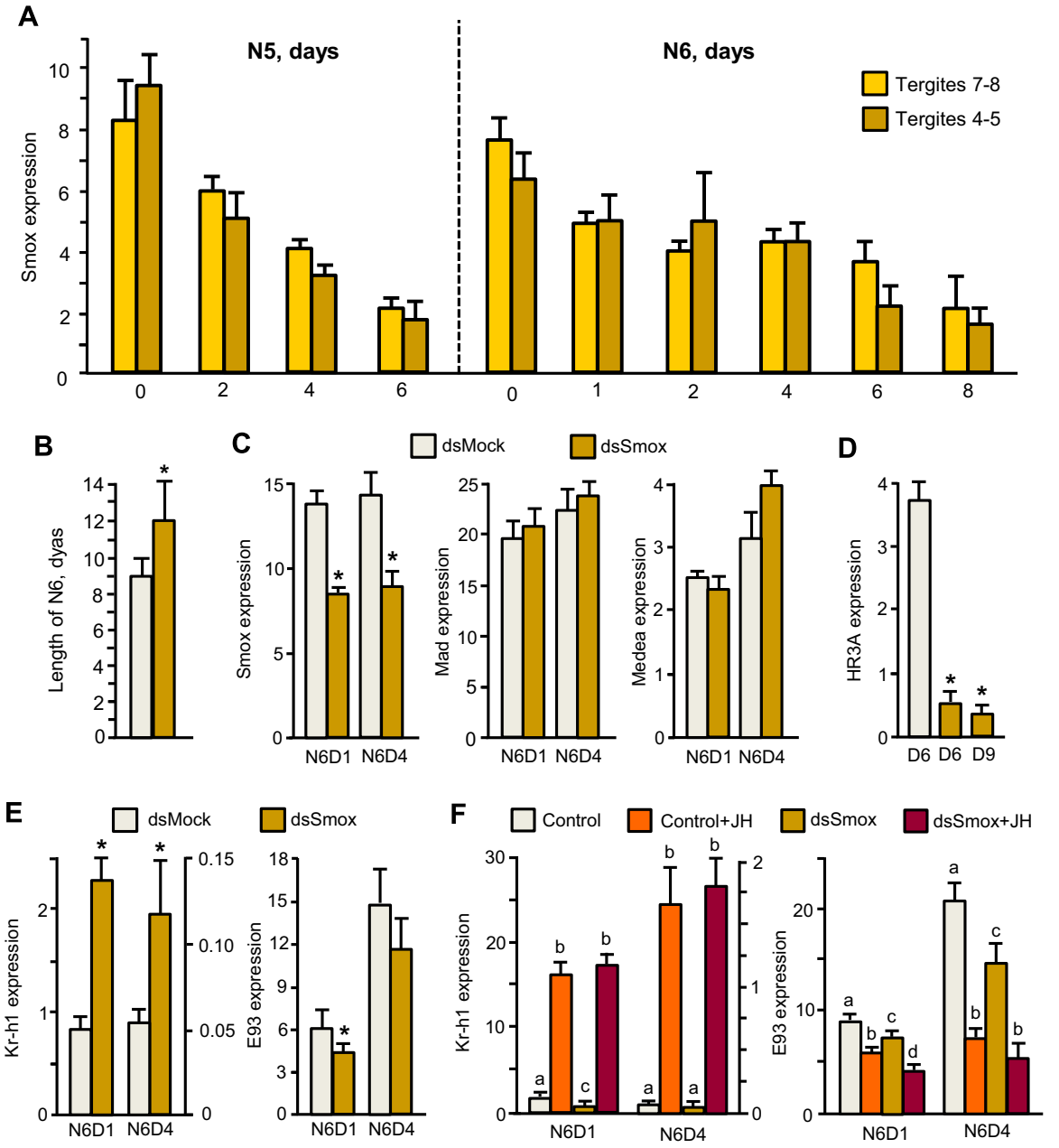

Fig. 2. Expression and function of Smox during metamorphosis of *Blattella germanica*. (A) Smox mRNA levels in fifth and sixth instars of male nymphs (N5 and N6, respectively), in tergites 7 and 8 and tergites 4 and 5. (B) Length of N6 (in days) in dsSmox-treated and control specimens; specimens were treated with two doses of 2 μg each of dsSmox on male nymphs, one on N5D0 and the other on N6D0. (C) Smox, Mad and Medea mRNA levels in dsSmox-treated and controls, measured on N6D1 and N6D4. (D) HR3A mRNA levels on N6D6. (E) Kr-h1 and E93 mRNA levels on N6D1 and N6D4. (F) Effects of JH treatment on Kr-h1 and E93 expression in Smox-depleted specimens; male nymphs freshly emerged to N6 received a 2-μg dose of dsSmox and were immediately treated with 10 μg of JHIII; controls for this experiment were equivalently treated with dsMock and JHIII; transcript levels were measured on N6D1 and N6D4; the scale or ordinates on the right of the Kr-h1 histograms in (E) and (F) applies for N6D4. From (C) to (F), mRNA levels were measured in the complete set of tergites. Each point of quantitative data in histograms represents between 3 and 4 biological replicates; results represent copies of the given transcript per 1000 copies of BgActin-5c mRNA and are expressed as the mean ± SEM; the asterisks in B, C, D and E indicate statistically significant differences with respect to controls, and different letters in F indicate statistically significant differences comparing all treatments; in all cases at $p < 0.05$ and according to the REST software tool (Pfaffl et al., 2002).

Results showed that the increase of Kr-h1 expression induced by JH was the same in dsMock- and dsSmox-treated specimens in both N6D0 and N6D4. Levels of E93 mRNA in this experiment were consistently low in dsSmox-treated specimens (Fig. 2F).

2.3. Depletion of Medea disrupts the MEKRE93 pathway and impairs adult morphogenesis

Following equivalent BLAST and PCR strategies, we obtained a cDNA corresponding to Medea, which had 1950 bp and comprised the complete ORF (GenBank accession number LN901332) that once translated gave a 650 amino acid protein containing the MH1 and MH2 domains typical of Smads and with significant sequence similarity to Medea proteins (top BLAST scores were obtained from Medea, or Smad4 orthologs of other organisms). In general, the mRNA levels of Medea were lower than those of Mad and Smox. In N5, the pattern was similar in all tergites: high levels of expression at the beginning of the stage and then a progressive decrease. In N6, transcript levels were more constant and generally higher in T7-8 than in T4-5 (Fig. 3A).

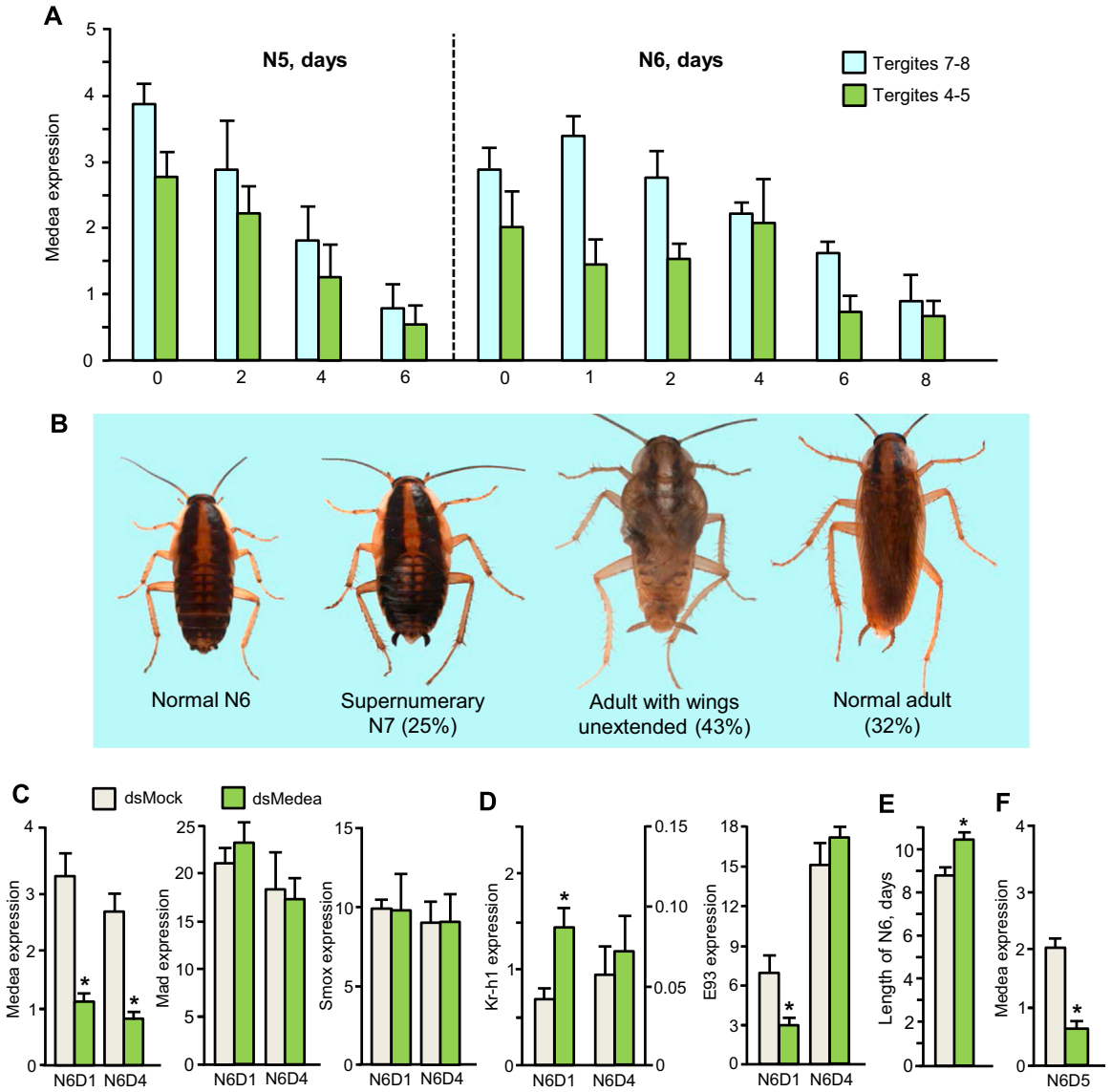

Fig. 3. Expression and function of Medea during metamorphosis of *Blattella germanica*. (A) Medea mRNA levels in fifth and sixth instars of male nymphs (N5 and N6, respectively), in tergites 7 and 8 and tergites 4 and 5. (B) Normal N6, normal adult, and phenotypes obtained with dsMedea treatments; specimens were treated with two doses of 2 μg each of dsMedea on male nymphs, one on N5D0 and the other on N6D0. (C) Medea, Mad and Smox mRNA levels in dsMedea-treated and controls, measured on N6D1 and N6D4. (D) Kr-h1 and E93 mRNA levels on N6D1 and N6D4; the scale or ordinates on the right of the Kr-h1 histogram applies for N6D4. (E) Length of N6 (in days) in dsMedea-treated and control specimens; in this experiment, specimens were treated with 2 μg of dsMedea on male nymphs on N6D3. (F) Medea mRNA levels in dsMedea-treated and controls of the former experiment, measured on N6D5. In panels (C), (D) and (F), mRNA levels were measured in the complete set of tergites. Each point of quantitative data in histograms represents between 3 and 4 biological replicates; results represent copies of the given transcript per 1000 copies of BgActin-5c mRNA and are expressed as the mean ± SEM; the asterisks indicate statistically significant differences with respect to controls ($p < 0.05$), according to the REST software tool (Pfaffl et al., 2002).

Again, we followed an RNAi approach to deplete Medea mRNA levels, using a dsRNA of 423 nucleotides designed on the linker region of Medea (dsMedea). We injected two 2 μg doses of dsMedea into male nymphs, one into freshly emerged penultimate instar (N5D0), and the other into freshly emerged final instar (N6D0). The controls received the same treatment but with dsMock. Phenotypically, all dsMock-treated specimens (n=41) molted to normal N6 and then to normal adults. All dsMedea-treated specimens (n=69) molted to normal N6, and then 17 specimens (25%) molted to a supernumerary nymph (N7), 30 (43%) had ecdysis problems but finally molted to adults that showed severely unextended wings (tegmina tile-shaped, generally not well extended, but especially in the apical part; membranous wings severely unextended, especially in the apical part), and 22 (32%) molted to normal adults (Fig. 3B). The length of N6 was between 8 and 9 days in controls and between 9 and 10 days in dsMedea-treated specimens, but the differences were not statistically significant. Transcript measurements carried out on N6D1 and N6D4 indicated that Medea mRNA levels were significantly reduced (an average of 68% and 70%, respectively) in dsMedea-treated specimens. Conversely, those of Mad and Smox were unaffected (Fig. 3C).

The results of measuring the mRNA levels of Kr-h1 and E93 on N6D1 and N6D4 showed that dsMedea treatment affected the decrease of Kr-h1 expression in N6D1, as the mRNA levels were significantly higher than those of controls (Fig. 3D). In N6D4, mRNA levels of Kr-h1 were very low both in controls and treated specimens (between 0.05 and 0.10 copies per 1000 copies of Actin-5c mRNA), but there was still a tendency for the levels to be higher in treated insects (Fig. 3D). In N6D1, levels of E93 mRNA were significantly lower in dsMedea-treated specimens than in controls, but practically normal levels were seen in N6D4 (Fig. 3C). These

effects on Kr-h1 and E93 were similar to those observed when depleting Smox, but in this case we obtained the supernumerary nymph phenotype and we did not observe the statistically significant molting delay found in the Smox experiments. We speculated that the effect of Medea was more marked in morphogenesis, especially due to the low levels of E93 in N6D1, and that these effects largely overrode the molting-delay phenotype. To test this conjecture, we implemented a treatment with 2 μg of dsMedea on N6N3 (n=16), once the expression of Kr-h1 had practically vanished and that of E93 was increasing normally (Belles and Santos, 2014). The controls (n=12) received an equivalent treatment with dsMock. As expected, these specimens molted to normal adults, but the molting of those treated with dsMedea was significantly delayed (2 days on average) with respect to the controls (Fig. 3E), although the adults were morphologically normal, as those resulting after depleting Smox. Examination of Medea expression on N6D5 revealed that this short-term RNAi treatment had been efficient (69% transcript reduction) (Fig. 3F).

2.4. Depletion of bursicon impairs wing extension

Bursicon (Burs) is a cystine knot protein that forms dimers composed by bursicon (α-subunit) and partner of bursicon (Pburs or ß-subunit), although in some cases they can also form homodimers (Honegger et al., 2008). In *B. germanica* we have recently described a bursicon sequence (Fernandez-Nicolas and Belles, 2016), and a blast search in the *B. germanica* genome assembly (https://www.hgsc.bcm.edu/arthropods/german-cockroach-genome-project) has led to find this sequence and that corresponding to Pburs (Scaffold705:1064492-1069290, amino acid translation: LQVQHVNLFTNLIFSEEFDDLGRLQRTCNGDVGVNKCE-GACNSQVQPSFFWILIYIFYQECYC-CRESFLRERTVTLTHCYDPDGGRLTKEGQATMDIRVRE-PADCKCFKCGDFSR), separated by 9.6 Kb from the bursicon sequence.

The typical phenotype showing unextended wings that resulted from Medea or Mad-depletion, suggested the involvement of Burs, given that this factor contributes to wing extension, as demonstrated in a number of insect species (Song, 2012). The first hint supporting this conjecture was that Burs mRNA levels in specimens treated with dsMad or dsMedea were lower than in controls (Fig. 4A). Then, we directly depleted Burs with RNAi, using a dsRNA of 311 nucleotides encompassing practically the entire fragment of Burs previously described (Accession number CUT08823.1). We injected a dose of 5 μg of dsBurs into freshly emerged final instar male nymphs (N6D0). The controls received the same treatment but with dsMock. Mock-treated specimens (n=12) molted to normal adults 8 days after the treatment (Fig. 4B). The dsBurs-treated specimens (n=18) molted to adults also 8 days after the treatment, but all them exhibited abnormal wings and tegmina. The mesothoracic tegmina were shorter than normal because the distal half had been not extended, longitudinally curled and tile-shaped. The metathoracic membranous wings were also only partially extended, especially in the posterior part, as in the case of tegmina. In both wing pairs, the venation was normal, at least in the extended part. There was certain variability, from relatively mild phenotypes, with only the proximal part of the tegmina and membranous wings extended (15 out of 18 specimens, Fig. 4C) to more severe phenotypes, with the tegmina deficiently extended in all their length or severely curled and the wings practically unextended (3 specimens, Fig. 4D and E). Transcript measurements were carried out on N6D7, which is the day were the insects complete the apolysis and one day before the ecdysis, when Burs would play its role of contributing to wing extension. Results indicated that Burs mRNA levels were significantly reduced (95% as average) with respect to controls (Fig. 4F).

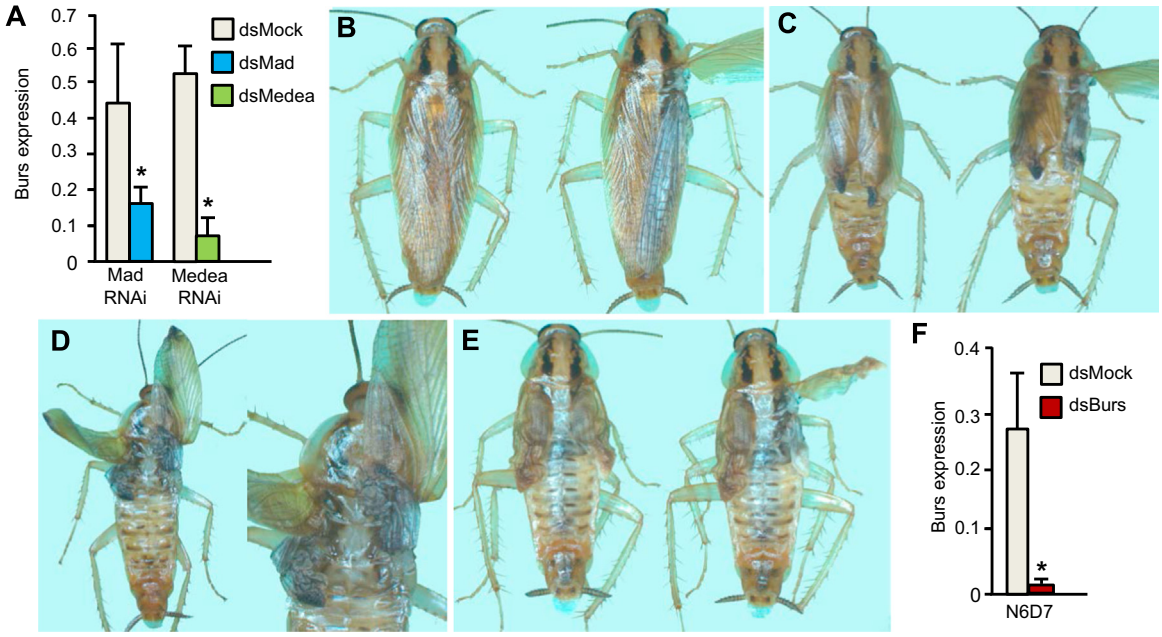

Fig. 4. Effects of Mad and Medea depletion on bursicon (Burs) mRNA levels, and role of Burs on wing extension in *Blattella germanica*. (A) Burs mRNA levels on N6D6 in Mad- and Medea-depleted specimens. (B). Control adult male in dorsal view. (C) Current phenotype of Burs-depleted adult males, with only the proximal part of the tegmina and membranous wings extended. (D,E). Severe phenotype of a Burs-depleted adult male, with the tegmina deficiently extended in all their length or severely curled and the wings practically unextended. In B-E the right image shows the metathoracic membranous wings, in B, C and E the right tegmina has been artificially opened to show these wings. (F) Burs mRNA levels on N6D7 in dsBurs-treated and dsMock-treated (control) specimens. In panels A and F, mRNA levels were measured in the complete set of tergites. Each point of quantitative data in histograms represents between 3 and 4 biological replicates; results represent copies of the given transcript per 1000 copies of BgActin-5c mRNA and are expressed as the mean ± SEM; the asterisks indicate statistically significant differences with respect to controls ($p < 0.05$), according to the REST software tool (Pfaffl et al., 2002).

3. Discussion

The problems of ecdysis and wing extension caused by Mad depletion led us to study the effects on HR3A, a gene of the ecdysone signaling pathway whose depletion in *B. germanica* triggers similar defects (Cruz et al., 2007). However, HR3A expression was not significantly affected in dsMad-treated specimens, thus suggesting that the defects observed were not due to problems of ecdysone signaling. Intriguingly, Mad-depleted specimens molted normally from N5 to N6, and showed ecdysis deficiencies only when molting to the adult stage. This suggests that the imaginal molt, which includes the extension of the tegmina and membranous wings from the wing pads, is mechanically more complex and possibly requires the contribution of specific factors related to proper wing extension, on which Mad has a regulatory role. It is worth noting that the unextended wings defect observed in Mad-depleted specimens is phenocopied in the Medea-depleted group.

The unextended or "inflated" wing phenotype led us to conjecture that Burs could have been affected by Mad depletion. Indeed, loss of BMP signaling in *D. melanogaster* affects the expression of several neuropeptides related to the regulation of molting, including bursicon, as well as crustacean cardioacceleratory peptide (CCAP) and myoinhibiting peptide (Mip) (Marques et al., 2003; Veverytsa and Allan, 2013). We assessed that Burs mRNA levels were lower in Mad-depleted specimens, which suggests that the dependence of Burs on the BMP pathway is conserved from cockroaches to flies. Then, we showed that direct RNAi of Burs triggers the typical "inflated wings" phenotype observed in the fruitfly *Drosophila melanogaster* (Dewey et al., 2004), the silkmoth *Bombyx mori* (Huang et al., 2007) and the flour beetle *Tribolium castaneum* (Arakane et al., 2008; Bai and Palli, 2010). This "inflated" wing phenotype of Burs-depleted specimens is reminiscent of the partially or totally unextended wings found in Mad- and Medea-depleted specimens. Thus, at least a part of the effect of Mad (and Medea) depletion on wing extension would be due to the effects on Burs.

The most apparent phenotype resulting from Smox depletion was the delayed imaginal molt. The length of N6 was 30% (3 days) longer, on average, in Smox-depleted specimens than in the controls. Interestingly, the length of N5 was unaffected, suggesting that the delay effect is specific to the final nymphal instar. This is reminiscent of the 2–3 day developmental delay in the formation of *D. melanogaster* puparium observed in zygotic mutants of babo, the type I receptor involved in the TGF-β/Activin branch of the TGF-β signaling pathway (Brummel et al., 1999). It is also similar to the more severe phenotype comprising 100% arrested development with no puparium formation observed after the suppression of activin signaling in the prothoracic gland, which impairs ecdysone production (Gibbens et al., 2011). Thus, the overall results suggest that in the final nymphal instar Smox is involved in regulating the timing of the imaginal molt, a role that appears conserved in *D. melanogaster*. Another result of Smox depletion is the disruption of the MEKRE93 pathway, concerning the expression of Kr-h1 and E93: the respective decrease and increase normally seen in N6D1 are impaired in dsSmox-treated specimens. Following an experimental design that had unveiled the co-activator role of CREB-binding protein on Kr-h1 (Fernandez-Nicolas and Belles, 2016), we simultaneously treated N6D0 with dsSmox and JH. This showed that the increase of Kr-h1 expression provoked by JH was the same in Smox depleted specimens and in controls, whereas E93 expression was consistently low. These results suggest that Smox does not act to co-repress Kr-h1, but rather contributing to the activation of E93. If so, then the higher Kr-h1 mRNA levels observed after depleting Smox would be due to the lower E93 expression, as E93 acts as a repressor of Kr-h1 (Belles and Santos, 2014; Ureña et al., 2014).

Intriguingly, the effect on impairing E93 expression increase and Kr-h1 expression decrease was similar in both the Smox- and Medea-depleted groups, but only the dsMedea treatment triggered a supernumerary N7 (in 25% of the specimens). We presume that these N7 obtained are mainly due to the relatively low levels of E93 expression on N6D1. Indeed, the mRNA levels of E93 were 28% lower in the case of dsSmox-treated insects compared with the controls, whereas E93 mRNA levels in dsMedea-treated specimens were 58% lower. It is perhaps this difference that determined the inhibition of metamorphosis in a quarter of the specimens in the Medea experiments. With respect to molting timing in the dsMedea depleted insects, in the group treated on N5D0 and N6D0 the length of N6 showed a tendency to increase, but in the group treated on N6D3, this length of time was significantly greater in the dsMedea-treated insects than in the controls. These results are fairly consistent with the molting delay phenotype observed in dsSmox-treated specimens.

In *D. melanogaster*, Mad is the R-Smad of the BMP branch of the TGF-β signaling pathway, Smox is the R-Smad of the TGF-β/Activin branch, and Medea participates in both branches in complex with Mad or Smox. We can presume that this division of pathways applies to *B. germanica* (we found no other R-Smads of Co-Smads in the genome of *B. germanica*) and in insects, in general. If so, then the most parsimonious hypothesis to explain the results reported in this study on the role of TGF-β signaling pathway in the metamorphosis of *B. germanica* is that the BMP branch is involved in the regulation of the imaginal ecdysis and wing extension, mainly through activating Burs, whereas the TGF-β/Activin branch, in addition to regulating the timing of the imaginal molt, contributes to controlling the increase of E93 (and the decrease of Kr-h1) at the beginning of the final nymphal instar, which is crucial for triggering adult morphogenesis (Fig. 5A).

The results for the TGF-β/Activin branch suggest that Smox-Medea acts as a co-activator of E93 at the beginning of the final nymphal instar, thus contributing to trigger metamorphosis. Smad factors co-activate or co-repress the expression of target genes by binding onto silencing or enhancing elements in the regulatory region of target genes (Muller et al., 2003; Pyrowolakis et al., 2004; Weiss et al., 2010). The motif AGAC has been identified as a typical of Smox binding site (Bai et al., 2013), whereas GTCT and GNCV are typical Medea binding sites (Gaarenstroom and Hill, 2014). Interestingly, the region of 5000 nucleotides upstream of the ORF of the *B. germanica* E93 gene, which should include the regulatory region, contains 18 AGAC as well as 11 GTCT and 122 GNCV motifs (not shown).

In *B. germanica*, the MEKRE93 pathway (Belles and Santos, 2014), in addition to JH and the transcription factors transducing their signal, involves additional modulatory roles of the microRNA miR-2, which scavenges Kr-h1 transcripts, thus contributing to decrease Kr-h1 expression, to increase E93 and to correctly trigger metamorphosis (Lozano et al., 2015), and a CREB-binding protein, that co-activates Kr-h1 transcription (Fernandez-Nicolas and Belles, 2016). Then, the present results show that the TGF-β/Activin branch of the TGF-β signaling pathway co-activates the expression of E93 and contributes to decrease Kr-h1 expression, thus adding a new layer of complexity and regulatory precision to the MEKRE93 pathway (Fig. 5B).

Finally, recent studies in the hemimetabolan species *Gryllus bimaculatus* have unveiled relevant roles of the TGF-β signaling pathways in development and metamorphosis related to the production of JH (Ishimaru et al., 2016). These studies show that high expression of the TGF-β ligand Myoglianin (which acts through the TGF-β/Activin branch) during the last nymphal instar induces metamorphosis through repressing the expression of the enzyme JH acid *O*-methyltransferase (JHAMT). JHAMT is the last and key enzyme of JH synthesis, thus high levels of Myoglianin

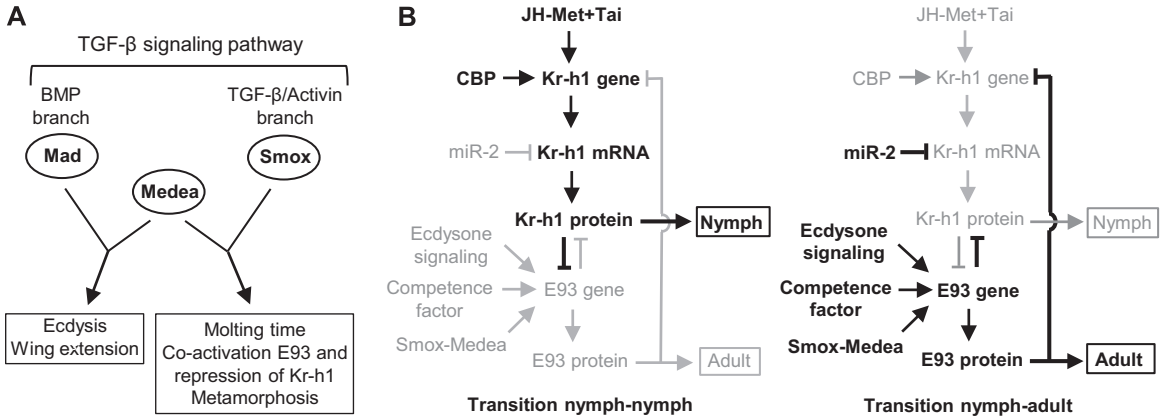

Fig. 5. The TGF-β signaling pathways in *Blattella germanica* metamorphosis. (A) Respective roles of the BMP and TGF-β/Activin branches. (B) Roles in the context of the MEKRE93 pathway; until the penultimate instar nymph (N5), juvenile hormone (JH) through Kr-h1, prevents metamorphosis; at the beginning of the final instar nymph (N6), JH production decreases (Treiblmayr et al., 2006), transcription of Kr-h1begins declining (Lozano and Belles, 2011), and the expression of E93, that had been repressed by Kr-h1 (Belles and Santos, 2014), begins increasing (Belles and Santos, 2014; Ureña et al., 2014). CREB-binding protein (CBP) co-activates Kr-h1 expression (Fernandez-Nicolas and Belles, 2016), and miR-2 contribute to remove Kr-h1 transcripts at the beginning of N6 (Lozano et al., 2015). Medea-Mad would co-activate the transcription of E93 (present results).

provoke a decline of JH, thus triggering metamorphosis. Conversely, JHAMT and JH production is up-regulated by the TGF-β ligands Decapentaplegic and Glass-bottom boat (which signal in the BMP branch) during nymphal stages, which keeps the status quo action of JH and prevents metamorphosis (Ishimaru et al., 2016). Arguably, these modulatory roles on JH production of the TGF-β signaling pathways could be extended to all insects (Ishimaru et al., 2016), which still add another regulatory layer upstream the MEKRE93 pathway, giving more robustness to the mechanisms regulating such an important process in insects as the metamorphosis.

4. Materials and methods

4.1. Insects

All *B. germanica* specimens used in the experiments were obtained from a colony reared in the dark at 30 ± 1 °C and 60–70% relative humidity. Freshly emerged male nymphs were selected and used at selected ages. Prior to injection treatments, dissections or tissue sampling, the experimental specimens were anaesthetized with carbon dioxide.

4.2. RNA extraction and retrotranscription to cDNA

We performed total RNA extraction from the whole body (excluding the digestive tube to avoid gut parasites) or specific tissues using the miRNeasy extraction kit (QIAGEN). A sample of 100–150 ng from each RNA extraction was treated with DNase (Promega) and reverse transcribed with first Strand cDNA Synthesis Kit (Roche) and random hexamers primers (Roche). RNA quantity and quality was estimated by spectrophotometric absorption at 260 nm using a Nanodrop Spectrophotometer ND-1000® (NanoDrop Technologies).

4.3. Cloning and sequencing Mad, Smox and Medea orthologs in B. germanica

To obtain the corresponding cDNAs of Mad, Medea and Smox, comprising the complete ORF, we combined BLAST search in *B. germanica* transcriptomes available in our laboratory (accession codes GSE63993, GSM1560373, GSM1560374, GSM1560375, SRX796238, SRX796239, SRX796244 and SRX790658), results of mapping these sequences in the *B. germanica* genome (https://www.hgsc.bcm.edu/arthropods/german-cockroach-genome-project) and PCR strategies to validate the transcriptome and genome sequences with RT-PCR using specific primers and cDNA from penultimate instar male nymphs of *B. germanica* as a template. All PCR products were subcloned into the pSTBlue-1 vector (Novagen) and sequenced.

4.4. Determination of mRNA levels by quantitative real-time PCR

Quantitative real time polymerase chain reactions (qRT-PCRs) were performed at least in triplicate in an iQ5 Real-Time PCR Detection System (Bio-Rad Laboratories), using SYBR®Green (Power SYBR® Green PCR Master Mix; Applied Biosystems). A

Table 1
Primers used to detect transcript levels by qPCR in *Blattella germanica* tissues and to prepare the dsRNAs for RNAi experiments.

Primer set	Forward primer (5′-3′)	Reverse primer (5′-3′)	Reference sequence
Mad	TCAACAGCCTTTTCTGCCCA	TGGATGCTGATGAAGCGGAA	LN901331
Medea	AGGTGTGGTGGGAGGTACTG	TTGTTTGAGGAACCGTGTGA	LN901332
Smox	GACACATTGGGAAAGGCGTT	GACTGTGATAAGAGCGCTGC	LT575495
HR3A	GATGAGCTGCTCTTAAAGGCGAT	AGGTGACCGAACTCCACATCTC	AM259128.1
Kr-h1	GCGAGTATTGCAGCAAATCA	GGGACGTTCTTTCGTATGGA	HE575250.1
E-93	TCCAATGTTTGATCCTGCAA	TTTGGGATGCAAAGAAATCC	HF536494.1
Bursicon	AATGGACGAGTGTCAGGTGACA	AACACATGCATGAACGTTCCAT	LN901328
dsMad	AGACAGGAGCAACTTCAGGC	ACCGTAAGGGCCTACCTCAT	LN901331
dsMedea	GTGGCCTCGCCTTCAAGTGC	ACCTGTCAGAGCAACATCTGATC	LN901332
dsSmox	TCACATGCAAGGAGTGGAGT	ACAGAAGGCAAAAGCACACA	LT575495
dsBurs	CTGCAATACCCAGGTTGTGTT	CTAAGGGGACCCTCATCAGC	LN901328

template-free control was included in all batches. The primers used to measure mRNA levels are described in Table 1. The efficiency of each set of primers was validated by constructing a standard curve through four serial dilutions. Levels of mRNA were estimated relative to BgActin-5c (Accession number AJ862721) expression, using the Bio-Rad iQ5 Standard Edition Optical System Software (version 2.0). Results are given as copies of mRNA per 1000 copies of BgActin-5c mRNA.

4.5. RNA interference

The detailed procedures followed for RNAi experiments were as described previously (Ciudad et al., 2006). The primers to generate the templates for the corresponding dsRNAs used for Mad, Medea, Smox and Burs are summarized in Table 1. The fragments were amplified by PCR and cloned into the pSTBlue-1 vector. A 307-bp sequence from *Autographa californica* nucleopoyhedrovirus (Accession number K01149) was used as control dsRNA (dsMock). The dsRNAs were prepared as reported by Ciudad et al. (2006). A volume of 1 μL of dsRNA solution (of a concentration between 2 and 4 μg/μL) was injected into the abdomen of the experimental specimens at chosen ages and stages with a 5-μL Hamilton microsyringe. Control specimens were equivalently treated with dsMock.

4.6. Treatment with juvenile hormone

In a series of experiments, dsSmox-treated specimens were further treated with JH III as follows. Male nymphs freshly emerged to N6 received a 2-μg dose of dsRNA (dsSmox or dsMock) and were topically treated with 10 μg of JH III (Sigma) in 2 μL of acetone. JH III is the native JH of *B. germanica* (Camps et al., 1987), and the commercial source used is a mixture of isomers containing ca. 50% of the biologically active (10*R*)-JH III, thus the active dose applied was around 5 μg per specimen, which is an effective dose that notably increases the expression of Kr-h1 (Fernandez-Nicolas and Belles, 2016; Lozano and Belles, 2011).

Contributions

C.G.S. and A.F.-N. carried out the experiments. C.G.S., A.F.-N. and X.B. designed the experiments and analyzed the data. X.B. wrote the manuscript. All the authors commented on the manuscript.

Acknowledgements

Thanks are due to the Spanish Ministry of Economy and Competitiveness (Grants CGL2012-36251 and CGL2015-64727-P, including FEDER funds, to X.B., and a predoctoral fellowship to A.F.-N.) and to the Catalan Government (2014 SGR 619). C.G.S. received a Grant from Brazil Government (Processo CNPQ, 24574812012-L) to work in the Institute of Evolutionary Biology in Barcelona. Thanks are also due to Guillem Ylla, for helping with transcriptome comparisons, and for searching the Pburs gene and the promoter region of the E93 gene in *B. germanica* genome, which is available at https://www.hgsc.bcm.edu/arthropods/german-cockroach-genome-project, as provided by the Baylor College of Medicine Human Genome Sequencing Center.

References

Arakane, Y., Li, B., Muthukrishnan, S., Beeman, R.W., Kramer, K.J., Park, Y., 2008. Functional analysis of four neuropeptides, EH, ETH, CCAP and bursicon, and their receptors in adult ecdysis behavior of the red flour beetle, *Tribolium castaneum*. Mech. Dev. 125, 984–995.

Bai, H., Palli, S.R., 2010. Functional characterization of bursicon receptor and genome-wide analysis for identification of genes affected by bursicon receptor RNAi. Dev. Biol. 344, 248–258.

Bai, H., Kang, P., Hernandez, A.M., Tatar, M., 2013. Activin signaling targeted by insulin/dFOXO regulates aging and muscle proteostasis in *Drosophila*. PLoS Genet. 9, e1003941.

Belles, X., 2011. Origin and evolution of insect metamorphosis. In: Encyclopedia of Life Sciences (ELS). John Wiley & Sons, Ltd., Chichester. http://dx.doi.org/10.1002/9780470015902.a0022854.

Belles, X., Santos, C.G., 2014. The MEKRE93 (Methoprene tolerant-Kruppel homolog 1-E93) pathway in the regulation of insect metamorphosis, and the homology of the pupal stage. Insect Biochem. Mol. Biol. 52, 60–68.

Brummel, T., Abdollah, S., Haerry, T.E., Shimell, M.J., Merriam, J., Raftery, L., Wrana, J. L., O'Connor, M.B., 1999. The *Drosophila* activin receptor baboon signals through dSmad2 and controls cell proliferation but not patterning during larval development. Genes Dev. 13, 98–111.

Camps, F., Casas, J., Sánchez, F.J., Messeguer, A., 1987. Identification of juvenile hormone III in the hemolymph of *Blattella germanica* adult females by gas chromatography–mass spectrometry. Arch. Insect Biochem. Physiol. 6, 181–189.

de Celis, J.F., Barrio, R., Kafatos, F.C., 1996. A gene complex acting downstream of dpp in *Drosophila* wing morphogenesis. Nature 381, 421–424.

Ciudad, L., Piulachs, M.D., Belles, X., 2006. Systemic RNAi of the cockroach vitellogenin receptor results in a phenotype similar to that of the *Drosophila* yolkless mutant. FEBS J. 273, 325–335.

Cruz, J., Martin, D., Belles, X., 2007. Redundant ecdysis regulatory functions of three nuclear receptor HR3 isoforms in the direct-developing insect *Blattella germanica*. Mech. Dev. 124, 180–189.

Dewey, E.M., McNabb, S.L., Ewer, J., Kuo, G.R., Takanishi, C.L., Truman, J.W., Honegger, H.W., 2004. Identification of the gene encoding bursicon, an insect neuropeptide responsible for cuticle sclerotization and wing spreading. Curr. Biol. 14, 1208–1213.

Fernandez-Nicolas, A., Belles, X., 2016. CREB-binding protein contributes to the regulation of endocrine and developmental pathways in insect hemimetabolan pre-metamorphosis. Biochim. Biophys. Acta 1860, 508–515.

Gaarenstroom, T., Hill, C.S., 2014. TGF-beta signaling to chromatin: how Smads regulate transcription during self-renewal and differentiation. Semin. Cell Dev. Biol. 32, 107–118.

Gibbens, Y.Y., Warren, J.T., Gilbert, L.I., O'Connor, M.B., 2011. Neuroendocrine regulation of *Drosophila* metamorphosis requires TGFbeta/Activin signaling. Development 138, 2693–2703.

Grimm, S., Pflugfelder, G.O., 1996. Control of the gene optomotor-blind in *Drosophila* wing development by decapentaplegic and wingless. Science 271, 1601–1604.

Heldin, C.H., Moustakas, A., 2012. Role of Smads in TGFbeta signaling. Cell Tissue Res. 347, 21–36.

Herpin, A., Lelong, C., Favrel, P., 2004. Transforming growth factor-beta-related proteins: an ancestral and widespread superfamily of cytokines in metazoans. Dev. Comp. Immunol. 28, 461–485.

Honegger, H.W., Dewey, E.M., Ewer, J., 2008. Bursicon, the tanning hormone of insects: recent advances following the discovery of its molecular identity. J. Comp. Physiol. A Neuroethol. Sens. Neural Behav. Physiol. 194, 989–1005.

Huang, J., Zhang, Y., Li, M., Wang, S., Liu, W., Couble, P., Zhao, G., Huang, Y., 2007. RNA interference-mediated silencing of the bursicon gene induces defects in wing expansion of silkworm. FEBS Lett. 581, 697–701.

Ishimaru, Y., Tomonari, S., Matsuoka, Y., Watanabe, T., Miyawaki, K., Bando, T., Tomioka, K., Ohuchi, H., Noji, S., Mito, T., 2016. TGF-beta signaling in insects regulates metamorphosis via juvenile hormone biosynthesis. Proc. Natl. Acad. Sci. USA 113, 5634–5639.

Itoh, S., ten Dijke, P., 2007. Negative regulation of TGF-beta receptor/Smad signal transduction. Curr. Opin. Cell Biol. 19, 176–184.

Jindra, M., Belles, X., Shinoda, T., 2015. Molecular basis of juvenile hormone signaling. Curr. Opin. Insect Sci. 11, 39–46.

Kim, J., Sebring, A., Esch, J.J., Kraus, M.E., Vorwerk, K., Magee, J., Carroll, S.B., 1996. Integration of positional signals and regulation of wing formation and identity by *Drosophila* vestigial gene. Nature 382, 133–138.

Lozano, J., Belles, X., 2011. Conserved repressive function of Kruppel homolog 1 on insect metamorphosis in hemimetabolous and holometabolous species. Sci. Rep. 1, 163.

Lozano, J., Belles, X., 2014. Role of Methoprene-tolerant (Met) in adult morphogenesis and in adult ecdysis of *Blattella germanica*. PLoS One 9, e103614.

Lozano, J., Montanez, R., Belles, X., 2015. MiR-2 family regulates insect metamorphosis by controlling the juvenile hormone signaling pathway. Proc. Natl. Acad. Sci. USA 112, 3740–3745.

Lozano, J., Kayukawa, T., Shinoda, T., Belles, X., 2014. A role for taiman in insect metamorphosis. PLoS Genet. 10, e1004769.

Marques, G., Haerry, T.E., Crotty, M.L., Xue, M., Zhang, B., O'Connor, M.B., 2003. Retrograde Gbb signaling through the Bmp type 2 receptor wishful thinking regulates systemic FMRFa expression in *Drosophila*. Development 130, 5457–5470.

Massague, J., 2012. TGFbeta signalling in context. Nat. Rev. Mol. Cell Biol. 13, 616–630.

Moustakas, A., Heldin, C.H., 2009. The regulation of TGFbeta signal transduction. Development 136, 3699–3714.

Muller, B., Hartmann, B., Pyrowolakis, G., Affolter, M., Basler, K., 2003. Conversion of

an extracellular Dpp/BMP morphogen gradient into an inverse transcriptional gradient. Cell 113, 221–233.
Nijhout, H.F., 1994. Insect Hormones. Princeton University Press, Princeton.
Peterson, A.J., O'Connor, M.B., 2013. Activin receptor inhibition by Smad2 regulates *Drosophila* wing disc patterning through BMP-response elements. Development 140, 649–659.
Peterson, A.J., O'Connor, M.B., 2014. Strategies for exploring TGF-beta signaling in *Drosophila*. Methods 68, 183–193.
Peterson, A.J., Jensen, P.A., Shimell, M., Stefancsik, R., Wijayatonge, R., Herder, R., Raftery, L.A., O'Connor, M.B., 2012. R-Smad competition controls activin receptor output in *Drosophila*. PLoS One 7, e36548.
Pfaffl, M.W., Horgan, G.W., Dempfle, L., 2002. Relative expression software tool (REST) for group-wise comparison and statistical analysis of relative expression results in real-time PCR. Nucleic Acids Res. 30, e36.
Pyrowolakis, G., Hartmann, B., Muller, B., Basler, K., Affolter, M., 2004. A simple molecular complex mediates widespread BMP-induced repression during *Drosophila* development. Dev. Cell 7, 229–240.
Romaña, I., Pascual, N., Belles, X., 1995. The ovary is a source of circulating ecdysteroids in *Blattella germanica* (L.) (Dictyoptera, Blattellidae). Eur. J. Entomol. 92, 93–103.
Song, Q., 2012. Bursicon, a neuropeptide hormone that controls cuticle tanning and wing expansion. In: Gilbert, L.I. (Ed.), Insect Endocrinology. Academic Press, London, pp. 93–105.
Szuperak, M., Salah, S., Meyer, E.J., Nagarajan, U., Ikmi, A., Gibson, M.C., 2011. Feedback regulation of *Drosophila* BMP signaling by the novel extracellular protein larval translucida. Development 138, 715–724.
Treiblmayr, K., Pascual, N., Piulachs, M.D., Keller, T., Belles, X., 2006. Juvenile hormone titer versus juvenile hormone synthesis in female nymphs and adults of the German cockroach, *Blattella germanica*. J. Insect Sci. 6, 1–7.
Ureña, E., Manjon, C., Franch-Marro, X., Martin, D., 2014. Transcription factor E93 specifies adult metamorphosis in hemimetabolous and holometabolous insects. Proc. Natl. Acad. Sci. USA 111, 7024–7029.
Veverytsa, L., Allan, D.W., 2013. Subtype-specific neuronal remodeling during *Drosophila* metamorphosis. Fly 7, 78–86.
Weiss, A., Charbonnier, E., Ellertsdottir, E., Tsirigos, A., Wolf, C., Schuh, R., Pyrowolakis, G., Affolter, M., 2010. A conserved activation element in BMP signaling during *Drosophila* development. Nat. Struct. Mol. Biol. 17, 69–76.
Ylla, G., Belles, X., 2015. Towards understanding the molecular basis of cockroach tergal gland morphogenesis. A transcriptomic approach. Insect Biochem. Mol. Biol. 63, 104–112.
Zheng, X., Wang, J., Haerry, T.E., Wu, A.Y., Martin, J., O'Connor, M.B., Lee, C.H., Lee, T., 2003. TGF-beta signaling activates steroid hormone receptor expression during neuronal remodeling in the *Drosophila* brain. Cell 112, 303–315.